Development of New Theoretical-Based Pedestal Temperature Model

T. Siriburanon and T. Onjun
Sirindhorn International Institute of Technology,
Thammasat University, Pathum Thani, 12121, Thailand
O. Onjun
[2]Department of Science Service, Ministry of Science and
Technology, Bangkok, 10400, Thailand

Abstract

A new predictive pedestal model based on theory-motivated models for the pedestal width and the pedestal pressure gradient is developed for the temperature at the top of the H-mode pedestal. A pedestal width model based on magnetic shear and flow shear stabilization is used in this study, where the pedestal pressure gradient is assumed to be limited by infinite n ballooning mode instability. The new pedestal model is implemented in the 1.5D BALDUR integrated predictive modeling code, where the same safety factor and magnetic shear are solved self-consistently and used in both core and pedestal models. With the self-consistent approach for calculating safety factor and magnetic shear, the effect of bootstrap current can be correctly included in the pedestal model. The pedestal model is used to provide the boundary conditions in the simulations and the Multi-mode core transport model is used to describe the core transport. This new integrated modeling protocol of the BALDUR code is used to predict the temperature and density profiles of 26 H-mode discharges. Simulations are carried out for 13 discharges in the Joint European Torus and 13 discharges in the DIII-D tokamak. The average root-mean-square deviation between experimental data and the predicted profiles of the temperature and the density, normalized by their central values, is found to be about 14%.

Keywords: Tokamak, H-mode, Pedestal, Stability

1. Introduction

It is known that when a plasma discharge is heated with sufficiently high heating power, it exhibits a spontaneous transition from a regime of confinement called low-mode (L-mode) to a regime with markedly improved confinement called high-mode (H-mode) [1]. The change in the plasma first appears at the edge of the plasma, where a region of steep gradients in temperature and density is formed. This steep gradient region, called the pedestal, is caused by a transport barrier that forms near the edge of the plasma. The pedestal region is important because the height of the pedestal strongly influences the confinement of the core plasma. It has been found in integrated modeling simulations that the same core transport model used in simulations of L-mode discharges can also be used in simulations of H-mode discharges, with equally good agreement with experimental data, as long as the simulation boundary conditions are given at the top of the pedestal at the edge of the H-mode discharges. It has also been found in both experiments and simulations of H-mode plasmas that the height of the pedestal has a significant impact on the shape of the temperature and density profiles and, consequently, a large effect on the global confinement scaling [2]. However, the need to use experimental data to provide temperature and density at the boundary of the integrated modeling simulations reduces the predictive capability of these simulations. Therefore, models are needed for the pedestal boundary conditions in order to make the integrated modeling simulations more predictive. It is important to develop more completely predictive integrated modeling codes in order to understand plasma confinement in present day tokamaks and to simulate new fusion experiments and future fusion reactor designs such as ITER.

Models that can be used to predict the temperature and density at the top of the pedestal have recently been developed and calibrated against experimental data [3-6]. In Ref. [3], several pedestal temperature models were developed using a theoretical approach. The magnetic shear and safety factor are calculated at one pedestal width away from the separatrix, where the safety factor profile is assumed. The predictions of the best model agree with experiment data with the root mean square error (RMSE) of 30%. Later, in Ref. [7], the pedestal temperature model in Ref. [3] was chosen to combine with predictive models for the core plasma to simulate existing tokamak experimental results. This pedestal model was implemented in the BALDUR integrated modeling code using an automated procedure to simulate the transition from the *L*-mode to *H*-mode, once the heating power rises above the *H*-mode threshold. When the plasma is in the *H*-mode state, the predicted values for the temperature and density at the top of the pedestal are used as boundary conditions in the simulations. The average relative root mean square (RMS) deviation between experimental data and the predicted profiles of temperature and density, normalized by central values, is found to be about 10%. Even though the protocol developed in Ref. [7] successfully reproduced various experimental data, the confidence in its predictions, especially when it is applied to a new plasma regime such as burning plasma experiment like ITER, is quite limited. One weak point of the protocol in Ref. [7] is the estimation of magnetic shear and safety factor in the pedestal temperature calculation, which is different from that used in the rest of the code. Note that the magnetic shear and safety factor play important roles in the maximum pedestal pressure gradient estimation. In addition, the pedestal temperature models in Ref. [3] were compared directly with the pedestal experimental data, which is known to contain high error values, in order to determine a pedestal width constant. In this work, we propose a new approach to develop a pedestal temperature model. This pedestal model is derived based on magnetic shear and flow shear stabilization and 1st ballooning mode pressure gradient limit. The magnetic shear and safety factor used in the pedestal model are taken directly from the BALDUR prediction, where the time-dependent equilibrium and plasma profile effects are properly included. Moreover, the pedestal width constant will be determined by minimizing the relative RMS deviation of the ion core temperature profile, which tends to be more accurate than the pedestal measurements.

This paper is organized as follows: Brief descriptions for a BALDUR integrated predictive modeling code, Multi-mode transport models, and pedestal models are given in Sec.2. A statistical analysis of the temperature and density profiles produced by simulation, using the MMM95 and the pedestal model together, compared with experimental data, is presented in Sec. 3, while conclusions are given in Sec. 4.

2. BALDUR Integrated Predictive Modeling Code

The BALDUR integrated predictive modeling code [8] is used to compute the time evolution of plasma profiles including electron and ion temperatures, deuterium and tritium densities, helium and impurity densities, magnetic q, neutrals, and fast ions. These time-evolving profiles are computed in the BALDUR integrated predictive modeling code by combining the effects of many physical processes self-consistently, including the effects of transport, plasma heating, particle influx, boundary conditions, the plasma equilibrium shape, and sawtooth oscillations. Fusion heating and helium accumulation are computed self-consistently. The BALDUR simulations have been intensively compared against various plasma experiments, which yield an overall agreement with 10% relative RMS deviation [9, 10]. In the BALDUR code, fusion heating power is determined using the nuclear reaction rates and a Fokker Planck package to compute the slowing down spectrum of fast alpha particles on each flux surface in the plasma [8]. The fusion heating component of the BALDUR code also computes the rate of the production of thermal helium ions and the rate of the depletion of deuterium and tritium ions within the plasma core. In this work, two core transport models in BALDUR will be used to carry out simulations of ITER. The brief details of these transport models are described below.

2.1 Multi-mode core transport model

The MMM95 model [11] is a linear combination of theory-based transport models

which consists of the Weiland model for the ion temperature gradient (ITG) and trapped electron modes (TEM), the Guzdar–Drake model for drift-resistive ballooning modes, as well as a smaller contribution from kinetic ballooning modes. The Weiland model for drift modes such as ITG and TEM modes usually provides the largest contribution to the MMM95 transport model in most of the plasma core. The Weiland model is derived by linearizing the fluid equations, with magnetic drifts for each plasma species. Eigenvalues and eigenvectors computed from these fluid equations are then used to compute a quasilinear approximation for the thermal and particle transport fluxes. The Weiland model includes many different physical phenomena such as effects of trapped electrons, $T_i \neq T_e$, impurities, fast ions, and finite β. The resistive ballooning model in MMM95 transport model is based on the 1993 **ExB** drift-resistive ballooning mode model by Guzdar–Drake [12], in which the transport is proportional to the pressure gradient and collisionality. The contribution from the resistive ballooning model usually dominates the transport near the plasma edge. Finally, the kinetic ballooning model is a semi-empirical model, which usually provides a small contribution to the total diffusivity throughout the plasma, except near the magnetic axis. This model is an approximation to the first ballooning mode stability limit. Since the models were originally derived for circular plasmas, all the anomalous transport contributions to the MMM95 transport model are multiplied by κ^{-4}, where κ is the elongation.

2.2 Pedestal models

A complete description of the pedestal model, based on magnetic and flow shear stabilization, that is used in this paper to predict the temperature at the top of the pedestal at the edge of the type I ELMy *H*-mode plasmas is given in Ref. [13]. In the development of the pedestal temperature models described in Ref. [3], two ingredients are required: the pedestal width (Δ) and the pedestal pressure gradient ($\partial p/\partial r$). If the pedestal density (n_{ped}) is known, the temperature at the top of the pedestal (T_{ped}) can be estimated as:

$$T_{ped} = \frac{1}{2n_{ped}k}\left|\frac{\partial p}{\partial r}\Delta\right| = \frac{\Delta}{2kn_{ped}}\frac{a_c B_T^2}{2\mu_0 R q^2}, \qquad (1)$$

where k is the Boltzmann constant, μ_0 is the permeability of free space, α_c is the normalized pressure gradient, B_T is the magnetic field, R is the major radius and q is the safety factor. Note that the notation is described in Table 1. The width of the pedestal is assumed to be determined by a combination of magnetic and flow shear stabilization of drift modes [13]:

$$\Delta = C_W \rho s^2, \qquad (2)$$

where C_W is a constant of proportionality, ρ is the ion gyroradius, and s is the magnetic shear. The pedestal pressure gradient is assumed to be uniform throughout the pedestal region and limited by the ballooning mode instability threshold, so that the normalized pressure gradient for the pedestal region is given by:

$$\alpha_c = 0.4s\left(1+\kappa_{95}^2\left(1+5\delta_{95}^2\right)\right), \qquad (3)$$

where s is the magnetic shear, κ_{95} is the elongation at the 95% flux surface, and δ_{95} is the triangularity at the 95% flux surface. Therefore, the pedestal temperature takes the following form:

$$T_{ped} = (keV) = 0.323 C_W^2 \left(\frac{B_T}{q^2}\right)^2 \left(\frac{M_i}{R^2}\right)\left(\frac{\alpha_c}{n_{ped,19}}\right)^2 s^4, \qquad (4)$$

where $n_{ped,19}$ is the electron density at the top of the pedestal in units of 10^{19} m^{-3}, and M_i is the ion mass. The constant C_W is the constant of proportionality in Eq. (2). The constant C_W is chosen so as to optimize the agreement between the experimental data of ion temperature profile and the simulation results for ion temperature profile by minimizing the relative RMS.

3. Results and Discussions

BALDUR integrated modeling simulations were carried out for the 26 H-mode discharges (13 JET and 13 DIII-D) in various scans from

DIII-D and JET tokamaks, using a combination of the new pedestal temperature model together with the MMM95 core transport model. These discharges are taken from the International Profile Database [14]. For simplicity, in this work, the electron pedestal temperature is assumed to be the same as the ion pedestal temperature. Note that this assumption is valid in high density plasma. In low plasma density, electron pedestal temperature is normally lower than ion pedestal temperature. The pedestal density is taken from the experiment in order to reduce an error from the density calculation. For each of the profiles (ion temperature, electron temperature, and electron density), the normalized deviation, ε_j , between the j_{th} experimental data point X_j^{exp} and the simulation result $X^{sim}(R_j)$ at the major radius R_j of the corresponding experimental data point is defined as:

$$\varepsilon_j = \frac{X^{sim}(R_j) - X_j^{exp}}{X_{Max}^{exp}} \qquad (5)$$

In order to give all the deviations across each profile equal weight, each deviation is normalized by the maximum experimentally measured value for that given profile, X_{Max}^{exp}. An alternative choice of normalizing each temperature deviation by the local temperature, for example, would magnify deviations near the edge of the plasma, where temperatures are lower. The RMS deviation σ and the offset f between the profile resulting from each simulation and the corresponding experimental data is defined as:

$$\sigma = \sqrt{\frac{1}{N}\sum_{j=1}^{N}\varepsilon_j^2} \qquad (6)$$

and

$$\text{Offset} = \frac{1}{N}\sum_{j=1}^{N}\varepsilon_j, \qquad (7)$$

where N is the number of experimental data points in a profile. The normalized RMS deviation (σ) and offset are evaluated for each of the temperature profiles for the discharges in consideration.

In Fig.1, the average relative RMS deviations for the ion temperature profiles of 26 H-mode discharges are plotted as a function of the pedestal width constant C_W. It can be seen that this function is close to a quadratic equation. When the fitting approach is used, the best fit with the quadratic equation is found to be:

$$\sigma(C_W) = 60.0C_W^2 - 56.1C_W - 27.4 \qquad (8)$$

The minimum point for the function in Eq.(8) can be found at the pedestal width constant of 0.47 and the lowest average RMS deviation is about 14.4%.

The details of the statistical analysis using relative RMS deviation for simulations using the pedestal model based on the magnetic and flow shear stabilization with C_W= 0.47 for ion and electron temperatures are presented in Figs. 2 and 3, respectively. Note that the DIII-D discharges are from discharge number 77557 to discharge number 99411 and the JET discharges are from discharge number 33131 to discharge number 38415. It can be seen in Fig. 2 that the relative RMS deviations for ion temperature vary from one discharge to another, and from the profile to another, with a minimum of about 3.56% and a maximum of about 37.82% for ion temperatures, and with a minimum of about 5.13% and a maximum of about 51.42% for electron temperatures. The average RMS deviation σ_{avg}, averaged over 26 discharges, for the ion temperature is about 14.39% for the ion temperature profiles and about 15.51% for the electron temperature profiles.

In Figs. 4 and 5, the relative offsets for simulations using the pedestal model with C_W= 0.47 are presented for ion and electron temperatures, respectively. It can be seen in Fig.4 that the offset for ion temperature also varies from one discharge to another, and from one profile to another, with a minimum of about -1.84% and a maximum of about 0.84% for ion temperatures and with a minimum of about -2.03% and a maximum of about 1.11% for electron temperatures. The average offset over 26 discharges for the ion temperature is about -0.20% for the ion temperature profiles and about 0.01% for the electron temperature profiles.

Profiles are shown in Figs. 6 and 7 from the simulations using the new pedestal model based on magnetic and flow shear stabilization compared with the experimental data for a discharge in the DIII-D elongation scan. Note that the DIII-D discharge 81499 is a low elongation discharge ($\kappa = 1.68$) while the DIII-D discharge 81507 is a high elongation discharge ($\kappa = 1.95$). It can be seen in Figs. 6 and 7 that the simulation profiles for ion temperature using the new pedestal model yield good agreement with experimental data. For Figs. 8 and 9, profiles from the simulations using the new pedestal model compared with experimental data for a discharge in the JET beta scan. Note that in the discharges 38407 and 38415, the plasma β, the ratio of plasma energy to magnetic energy, was varied by a factor of 1.5 while holding ρ^* and the dimensionless collisionality fixed. It can be seen in Figs. 8 and 9 that the simulation profiles for the ion temperature using the new pedestal model yield good agreement with experimental data. As shown in Figs. 6 - 9, the conditions at the boundary of the simulations that used the new pedestal model nearly match the corresponding experimental data. Consequently, the differences between the simulated profiles and the experimental data are the result of the core models used in the simulations—either the core transport model or the models used for sources and sinks.

4. Conclusions

A new protocol is being developed for predicting the temperature and density profiles in H-mode plasmas, where the same values of magnetic shear and safety factor are used in both core and pedestal models. As a result, stability effects can be properly included in the pedestal calculation. This protocol is used to compare profiles with experimental data from 26 discharges in the JET and DIII-D tokamaks. When the results of the simulations using this protocol are compared with experimental data from 26 JET and DIII-D H-mode discharges, it is found that the average relative RMS deviation is approximately 14.39% for the ion temperature profiles and 15.51% for the electron temperature profiles. The average relative offset is approximately -0.20% for the ion temperature profiles and 0.01% for the electron temperature profiles. When the experimentally measured profiles are compared with the profiles computed using this protocol, the agreement is worse than the agreement obtained when experimental data is used to provide the boundary conditions for the simulations (rather than a predictive pedestal model).

5. Acknowledgements

T. Onjun is grateful to Prof. Arnold H. Kritz, Dr. Glenn Bateman and Dr. Alexei Pankin for their generous support. This work is supported by National Research Council of Thailand, Thailand Toray Science Foundation, and Thammasat University Research Fund.

6. References

[1] Wagner, F., *et al.* Regime of Improved Confinement and High Beta in Neutral-Beam-Heated Divertor Discharges of the ASDEX Tokamak, Phys. Rev. Lett., Vol. 49, pp. 1408-1412, 1982

[2] Greenwald, M., *et al.* H-mode confinement in Alcator C-Mod, Nucl. Fusion, Vol. 37, pp. 793-808, 1997

[3] Onjun, T., Bateman, G., Kritz, A.H. and Hammett, G., Models for the pedestal temperature at the edge of H-mode tokamak plasmas, Physics of Plasmas, Vol. 9, pp. 5018-5030. 2002

[4] Onjun, T., Pedestal temperature models based on first and second stability limits of ballooning modes, Laser and Particle Beams, Vol. 24, pp. 113-116, 2006

[5] Guzdar, P. N., Mahajan, S. M., and Yoshida, Z., A theory for the pressure pedestal in high (H) mode tokamak discharges, Physics of Plasmas, Vol. 12, p. 032502, 2005

[6] Stacey, W. M., An Edge Pedestal Model, Contrib. Plasma Phys., Vol. 42, pp. 283-289, 2002

[7] Bateman, G, Onjun, T., and Kritz, A. H., Integrated predictive modelling simulations of burning plasma experiment designs, Plasma Phys. Control. Fusion, Vol. 45, pp. 1939-1960, 2003

[8] Singer, C. E., *et al.* Baldur: A one-dimensional plasma transport code., Comput. Phys. Commun., Vol. 49, pp. 275-398, 1988

[9] Hannum, D., *et al.*, Comparison of high-mode predictive simulations using Mixed

Bohm/gyro-Bohm and Multi-Mode MMM95 transport models, Physics of Plasmas, Vol. 8, pp. 964-974, 2001

[10] Onjun, T., *et al.*, Comparison of low confinement mode transport simulations using the mixed Bohm/gyro-Bohm and the Multi-Mode-95 transport model, Physics of Plasmas, Vol. 8, pp. 975-985, 2001

[11] Bateman, G., *et al.* Predicting temperature and density profiles in tokamaks, Physics of Plasmas, Vol. 5, pp. 1793-1799, 1998

[12] Guzdar, P. N., *et al.*, Three-dimensional fluid simulations of the nonlinear drift-resistive ballooning modes in tokamak edge plasmas, Phys. Fluids B, Vol. 5, pp. 3712-3727, 1993

[13] Sugihara, M., *et al.*, A model for H-mode pedestal width scaling using the International Pedestal Database, Nuclear Fusion, Vol. 40, pp. 1743-1756, 2000

[14] Boucher, D., *et al.*, The International Multi-Tokamak Profile Database, Nuclear. Fusion, Vol. 40, pp. 1955-1982, 2000

Table 1: Notation used in this paper

Symbol	Unit	Description
a	m	Plasma minor radius (half-width)
r	m	Flux surface minor radius (half-width)
R	m	Major radius to geometric center of each flux surface
κ		Plasma elongation
δ		Plasma triangularity
B_T	Tesla	Vacuum toroidal magnetic field at R
I_p	MA	Toroidal plasma current
Mi	AMU	Hydrogenic mass
n_e	m^{-3}	Electron density
T_e	keV	Electron temperature
T_i	keV	Ion temperature
β		Beta $[k_b(n_eT_e+n_iT_i)/(B_T{}^2/2\mu_o)]$
ρ	m	Ion gyroradius
s		Magnetic shear
q		Safety factor

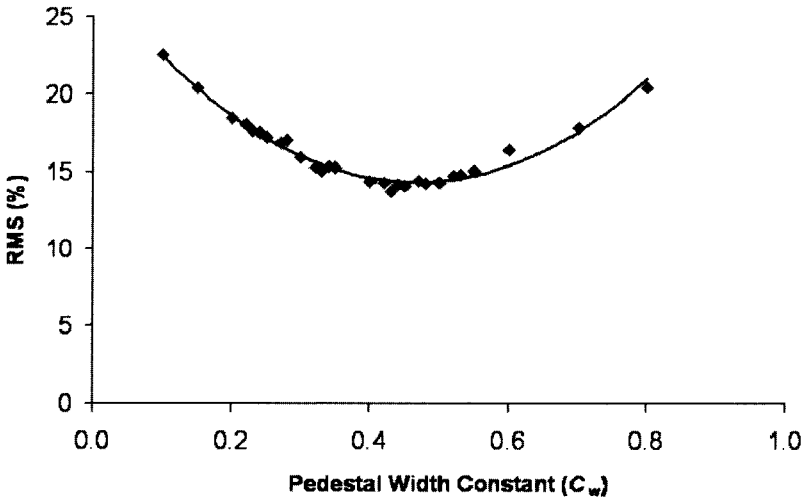

Fig. 1: The average relative RMS deviation for the ion temperature is plotted as a function of the pedestal width constant C_W.

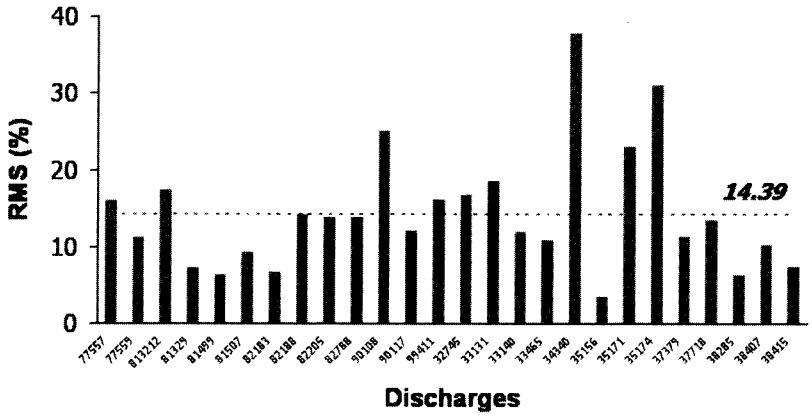

Fig. 2: Relative RMS deviations (%) for the ion temperature profiles produced by simulations using the MMM95 transport model combined with the pedestal model (using C_W=0.47) compared with experimental data for 26 H-mode discharges from DIII-D and JET experiments.

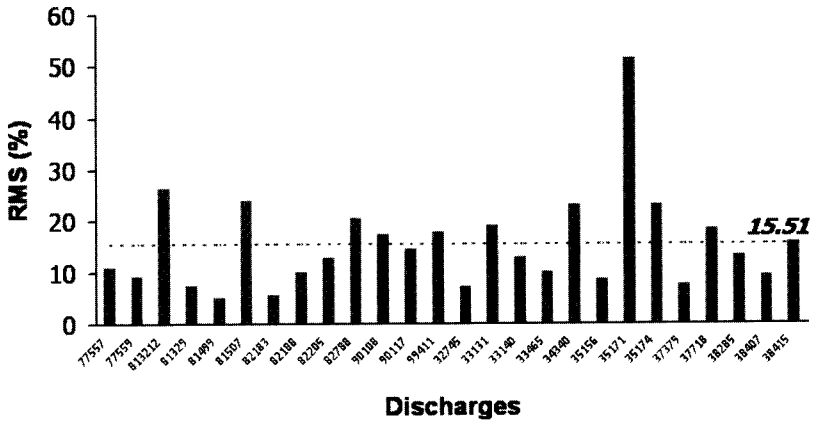

Fig. 3: Relative RMS deviations (%) for the electron temperature profiles produced by simulations using the MMM95 transport model combined with the pedestal model (using C_W=0.47) compared with experimental data for 26 H-mode discharges from DIII-D and JET experiments.

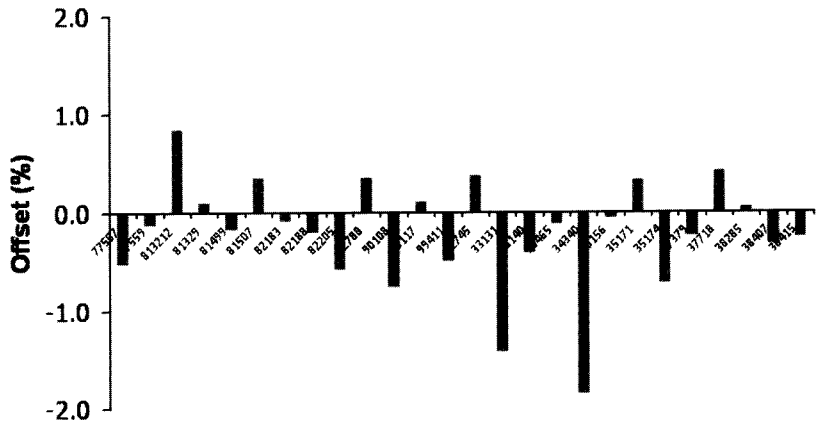

Fig. 4: Relative offset (%) for the ion temperature profiles produced by simulations using the MMM95 transport model combined with the pedestal model (using C_W=0.47) compared with experimental data for 26 H-mode discharges from DIII-D and JET experiments.

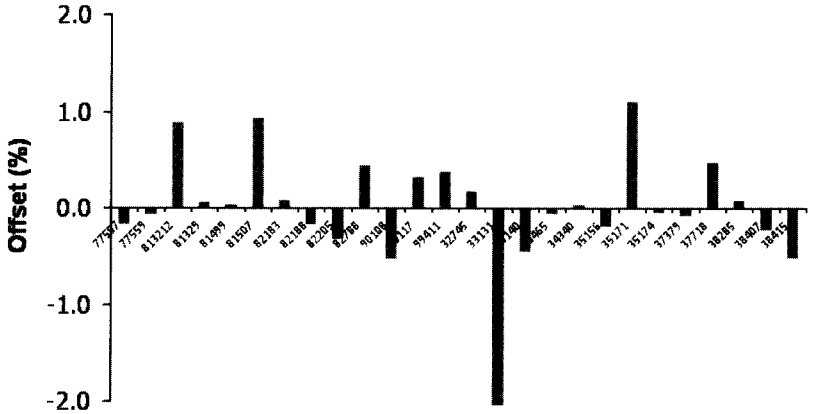

Fig. 5: Relative offset (%) for the electron temperature profiles produced by simulations using the MMM95 transport model combined with the pedestal model (using C_W=0.47) compared with experimental data for 26 H-mode discharges from DIII-D and JET experiments.

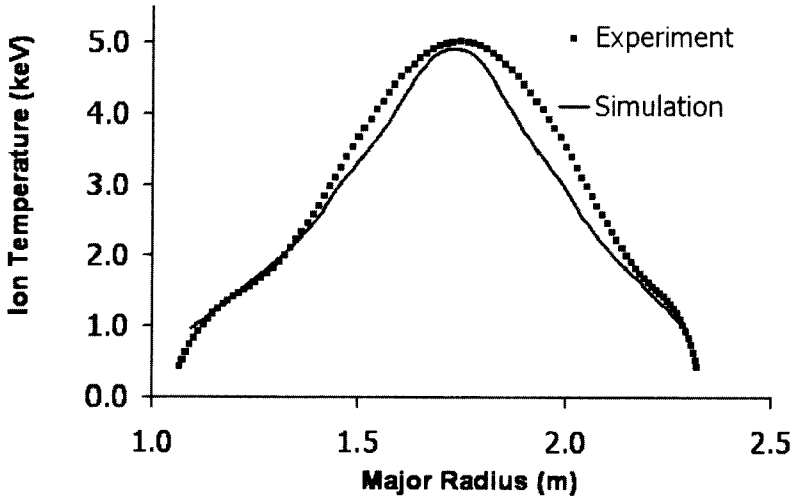

Fig. 6: The ion temperature profile is shown as a function of major radius for simulations of the low κ DIII-D discharge 81499. The closed squares represent experimental data, while the solid curve is the result of simulation.

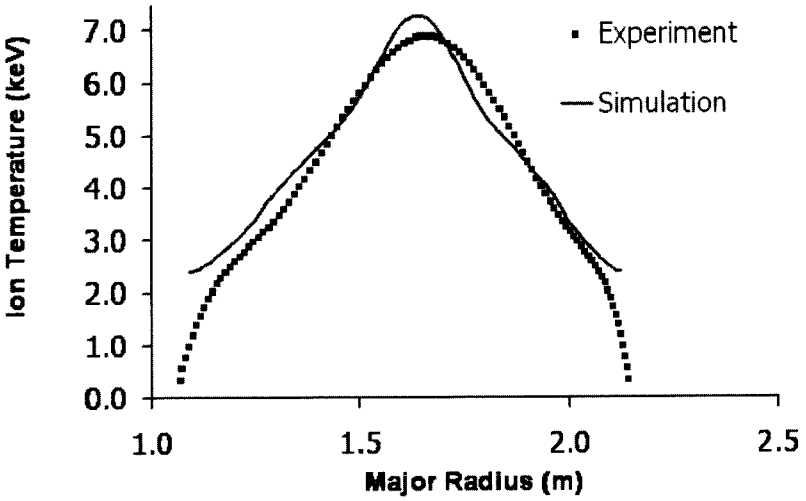

Fig. 7: The ion temperature profile is shown as a function of major radius for simulations of the high κ DIII-D discharge 81507. The closed circles represent experimental data, while the solid curve is the result of simulation.

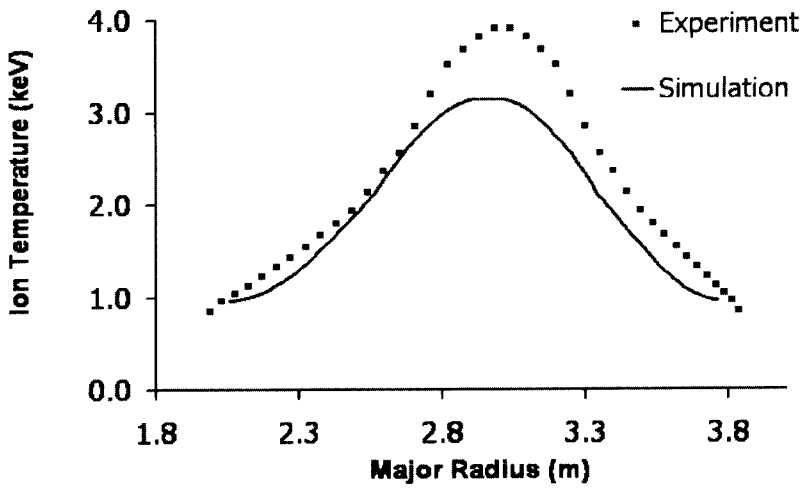

Fig. 8: The ion temperature profile is shown as a function of major radius for simulations of the low β JET discharge 38407. The closed circles represent experimental data, while the solid curve is the result of simulation.

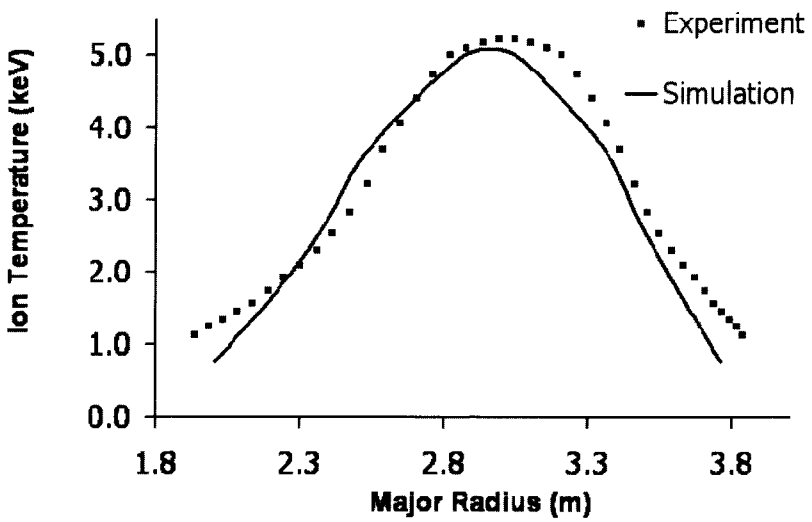

Fig. 9: The ion temperature profile is shown as a function of major radius for simulations of the high β JET discharge 38415. The closed circles represent experimental data, while the solid curve is the result of simulation.